

Article

Robust LQR Control for PWM Converters with Parameter-Dependent Lyapunov Functions

Nedia Aouani ¹  and Carlos Olalla ^{2,*} 

¹ Research Unit of System Analysis and Control, National School Engineering of Tunis, B.P. 37, Le Belvédère, Tunis 1002, Tunisia; nadia.aouani@ensta.u-carthage.tn

² Departament d'Enginyeria Elèctrica, Electrònica i Automàtica, Universitat Rovira i Virgili, 43007 Tarragona, Spain

* Correspondence: carlos.olalla@urv.cat; Tel.: +34-977-558-632

Received: 30 September 2020; Accepted: 23 October 2020; Published: 26 October 2020



Abstract: This paper presents a novel framework for robust linear quadratic regulator (LQR)-based control of pulse-width modulated (PWM) converters. The converter is modeled as a linear parameter-varying (LPV) system and the uncertainties, besides their rate of change, are taken into account. The proposed control synthesis method exploits the potential of linear matrix inequalities (LMIs), assuring robust stability whilst obtaining non-conservative results. The method has been validated in a PWM DC–DC boost converter, such that it has been shown, with the aid of simulations, that improved robustness and improved performance properties can be achieved, with respect to previously proposed approaches.

Keywords: uncertainty; PWM converters; LQR; LMIs; robustness; performance

1. Introduction

Control systems for power converters typically must satisfy several specifications and requirements, while dealing with uncertainty or operating point dependence at the same time. Since worst-case models may not exist or be different for each specification, the conventional industry standard approaches, such as the ones based on voltage-mode [1,2] and current-mode [2–4] controllers, rely on expert knowledge, simulation and iteration in order to find an appropriate controller.

As an alternative to this manual iteration, the automatic synthesis of controllers for switched-mode power converters has been one active topic of research in the last decade. These approaches are of interest because they can take into account the requirements together with the uncertainty or the nonlinearities of the converter to provide robust stability and performance, and they can do all that by imposing conditions beforehand.

Methods based on linear matrix inequalities (LMIs) have been some of the most successful approaches to the synthesis of robust controllers for power converters. The first attempts [5–7] demonstrated how uncertainty could be modeled and how the transient and frequency domain specifications could be taken into account. More recently, the efforts have been focused on approaches that do not require full state feedback [8], that improve the robustness [9] or the performance properties [10]. Although these papers employ averaged models of the converters, other approaches have also tackled the problem from a hybrid system perspective [11,12].

One of the open problems in the topic is the fact that the results may be conservative. The synthesized controller may not offer the best possible performance, when compared with conventionally tuned controllers, such as current-mode controllers. One possible solution to this conservativeness was shown in [13], where excellent robustness and tight regulation were achieved simultaneously, at the expense of control complexity.

One of the causes behind the conservativeness of LMI methods in [7] is the fact that the stability of the system is ensured no matter how large the derivative of the uncertain parameters may be. Specifically, when the uncertainty is characterized by being norm bounded, time varying and evolving in a set of polyhedral vertices, one difficulty remains: how to find an adequate mathematical representation for it, as well as for its rate of variation [14]. Nonetheless, several ways for representing both the derivative of the time-dependent parameter and the parameter itself have been proposed in the literature [14–17]. Different approaches to control these uncertain systems have been reported, such as state feedback gain-scheduling control [18], output feedback [15], linear quadratic Gaussian (LQG) or linear quadratic regulator (LQR) controllers [19–21] and gain-scheduled linear quadratic regulators (LQRs) [22,23].

In this paper, we propose a new method to synthesize robust LQR controllers for pulse-width modulated (PWM) converters, with the objective to improve the LQR synthesis that was proposed in [7]. The method is based on the results introduced in [14,15], such that the proposed approach can consider the time derivative of the uncertain parameters. As a consequence, the new LQR formulation can obtain less conservative results. This reduced conservativeness can be seen as a new degree of freedom. With this method, practicing engineers can synthesize controllers for larger sets of uncertainty (i.e., with improved robustness) or controllers that provide tighter regulation (i.e., improved performance) when compared with the previous method. The approach has been verified with the synthesis of a controller for a boost converter, such that a direct comparison with [7] has been carried out. Note that the proposed method could also be used in other switched-mode power converters, such as the buck converter (which was also treated in [7]).

This paper is organized as follows. Section 2 briefly reviews the modeling of the boost converter and the LQR state feedback proposed in [7]. Then, Section 3 proposes a new formulation of the LQR problem, such that novel LMI conditions are given. In Section 4, the proposed synthesis method is employed in the boost converter, using the original model and other alternatives that allow us to obtain improved robustness or improved performance. The appropriateness of the approach is verified with simulations in Section 5. Finally, conclusions are given in Section 6.

2. Modeling of the DC–DC Converter and LQR State Feedback Control

This section introduces the state feedback control approach proposed in [7], which resulted in the automatic synthesis of robust LQR controllers for PWM power converters.

2.1. Averaged Model of the DC–DC Boost Converter

Figure 1 shows the block diagram of a DC–DC converter with the control subsystem, where $v_0(t)$ is the output voltage, $v_g(t)$ is the line voltage, $i_{load}(t)$ is the load disturbance. The output voltage must be kept at a given value V_{ref} . The converter load is modeled as a resistor R .

In [7], the averaged model of a boost converter is given in the form

$$\dot{x}(t) = A(\theta)x(t) + B_u(\theta)u(t) \tag{1}$$

The uncertainty in $A(\theta)$ and $B_u(\theta)$ is included in a convex polytope as follows:

$$\begin{aligned} [A(\theta), B_u(\theta)] &\in \text{Co}\{\zeta_1, \dots, \zeta_N\} \\ &:= \left\{ \sum_{i=1}^N \lambda_i \zeta_i, \lambda_i \geq 0, \sum_{i=1}^N \lambda_i = 1 \right\} \end{aligned} \tag{2}$$

In general, the admissible values of vector θ are constrained in an hyperrectangle in the parameter space \mathfrak{R}^N .

The images of the matrix $[A(\theta), B_u(\theta)]$ for each vertex v_i correspond to a set $\{\zeta_1, \dots, \zeta_N\}$. The components of the set $\{\zeta_1, \dots, \zeta_N\}$ are the extrema of a convex polytope which contains the images for all admissible values of θ if the $[A(\theta), B_u(\theta)]$ depends linearly on θ [7].

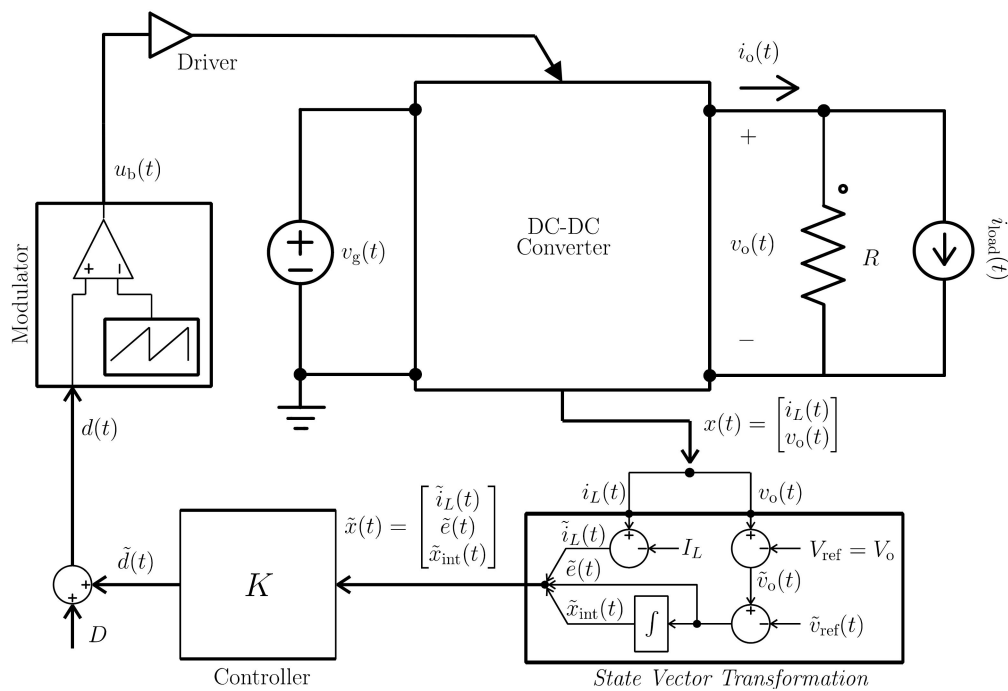


Figure 1. Schematic of a DC–DC converter with a state feedback control subsystem.

Where

$$A(\theta) = \begin{bmatrix} \frac{-R_L}{L} & -\frac{D'}{L} & 0 \\ \frac{D'}{C} & -\frac{1}{RC} & 0 \\ 0 & -1 & 0 \end{bmatrix}; \quad B_u(\theta) = \begin{bmatrix} \frac{V_g}{D'L} \\ -\frac{V_g}{(D'^2R)C} \\ 0 \end{bmatrix} \tag{3}$$

According to [7], for the DC–DC boost converter, the load R and the duty cycle D'_d at the operating point are considered uncertain parameters. Besides, two new uncertain variables, $\delta = \frac{1}{D'_d}$ and $\beta = \frac{1}{D'^2_d R'}$, are defined. Thus, the parameter vector was defined as:

$$\theta = \left[\frac{1}{R} \quad D'_d \quad \delta \quad \beta \right] \tag{4}$$

where the components of the parameter vector are restricted inside the following intervals:

$$\begin{aligned} R &\in \left[\frac{1}{R_{\max}}, \frac{1}{R_{\min}} \right] \\ D'_d &\in \left[D'_{d\min}, D'_{d\max} \right] \\ \delta &\in \left[\frac{1}{D'_{d\max}}, \frac{1}{D'_{d\min}} \right] \\ \beta &\in \left[\frac{1}{(D'_{d\max})^2 R_{\max}}, \frac{1}{(D'_{d\min})^2 R_{\min}} \right] \end{aligned} \tag{5}$$

This gives an uncertain model, which from now on is noted as P_{2009} , inside a polytopic domain formed by $N = 2^4$ vertices. A three-dimensional representation of P_{2009} is shown in Figure 2. This model was used in [7] to synthesize a robust LQR controller, as is explained in the next subsection.

2.2. Previous LMI Formulation of the LQR Synthesis Problem

In [7], the LQR problem was solved as follows:

$$\begin{aligned} & \min_{P,Y,X} Tr(QP) + Tr(X) \\ \text{Subject to} & \\ & A_i P + P A_i^T + B_{ui} Y + Y^T B_{ui}^T + I < 0 \\ & \begin{bmatrix} X & R^{\frac{1}{2}} Y \\ Y R^{\frac{1}{2}} & P \end{bmatrix} > 0 \\ & P > 0 \text{ For } i = 1, \dots, N \end{aligned} \tag{6}$$

N is the number of vertices of the polytope. Q and R are constant matrices that set weights on states and control effort. Once this minimization under constraints is solved, the optimal LQR controller was recovered by $K = YP^{-1}$.

In the next section, we aim to establish new LMI formulation for an LQR problem treating linear systems with time-varying parameters.

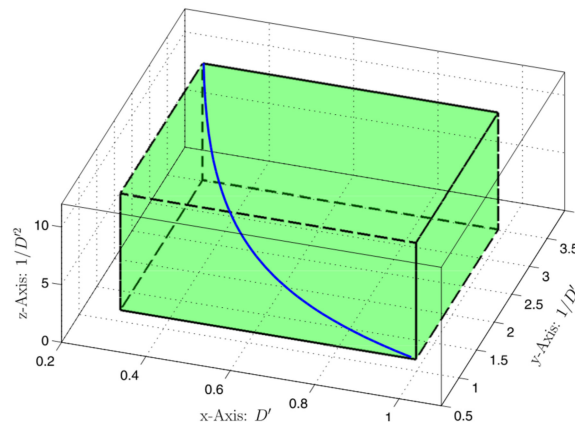


Figure 2. Plot of nonlinear uncertainty function ($f(D'')$) (solid line) and three-dimensional projection of the polytope P_{2009} (dashed line), as in [7].

3. New Formulation of the LQR Problem for Linear Parameter-Varying (LPV) Polytopic Systems

3.1. Proposed Representation of Uncertainty and Its Rate of Variation

Let us consider the continuous linear parameter time-dependent system, given by the state representation:

$$\dot{x}(t) = A(\theta(t))x(t) + B_u(\theta(t))u(t) \tag{7}$$

where $x(t) \in \mathfrak{X}^n$ is the state and $u(t) \in \mathfrak{X}^m$ is the input.

We assume the system matrices $A(\theta(t))$ and $B_u(\theta(t))$ are dependent on the parameter $\theta_i(t)$, i.e.,

$$A(\theta(t)) = \sum_{i=1}^N \theta_i(t) A_i \tag{8}$$

$$B_u(\theta(t)) = \sum_{i=1}^N \theta_i(t) B_{ui} \tag{9}$$

where A_i and B_i are now constant matrices ($i = 1..N$).

The time-varying parameter $\theta(t)$ varies in a polytope given by:

$$\theta(t) \in \Lambda_N, \text{ where } \Lambda_N := \left\{ \theta \in \mathfrak{R}^N : \sum_{i=1}^N \theta_i = 1, 0 \leq \theta_i \leq 1 \right\} \tag{10}$$

N is, again, the number of vertices of the polytope.

Its time derivative $\dot{\theta}(t)$ is such that:

$$\|\dot{\theta}(t)\| \leq b; \quad b \geq 0 \tag{11}$$

b is a positive real number that bounds the parameter's derivative.

If the uncertain parameter θ_i belongs to the set given by (10) and satisfies (11), then its time derivative can be written as [14,15]:

$$\dot{\theta}_i = r(\sigma_j - \beta_k) \tag{12}$$

σ_j and β_k belong, respectively, to the polytopes given by:

$$\sigma(t) \in \Lambda_M; \quad \Lambda_M := \left\{ \sigma \in \mathfrak{R}^M : \sum_{j=1}^M \sigma_j = 1, 0 \leq \sigma_j \leq 1 \right\} \tag{13}$$

$$\beta(t) \in \Lambda_K; \quad \Lambda_K := \left\{ \beta \in \mathfrak{R}^K : \sum_{k=1}^K \beta_k = 1, 0 \leq \beta_k \leq 1 \right\} \tag{14}$$

3.2. New LQR Problem Formulation for Uncertain LPV System

We are interested in an LMI formulation of the LQR problem adapted from [7]. Given the system presented in (1), the optimal LQR controller is obtained by using the state feedback gain K ($u = Kx$) that minimizes a performance index.

$$J = \int_0^{\infty} (x^T Q x + u^T R u) dt \tag{15}$$

where Q is a symmetric and semidefinite positive matrix and R is a symmetric and definite positive matrix.

The pair (A, Bu) must be controllable. The LQR problem can be viewed as the weighted minimization of a linear combination of the state x and the control input u . The weighting matrix Q establishes which states are to be controlled more tightly than others. R weights the amount of control action to be applied depending on how large the deviation of the state x is [7]. This optimization of cost weight constrains the magnitude of the control signal. The LQR controller is obtained by using the feedback gain K such that, in closed loop, the performance index (15) is rewritten:

$$J = \int_0^{\infty} (x^T (Q + K^T R K) x) dt \tag{16}$$

In this paper, we aim to give an LMI formulation for the same LQR problem as in [7], taking into account the uncertain parameter $\theta(t)$ that evolves into (10). We also consider the time derivative of this parameter as it is expressed in (12). The novel LQR formulation for the LPV system is given in the following theorem.

Theorem 1. The complete LMI formulation of the LQR problem is: considering system (7), in the uncertain domains (10)–(11), with N symmetric and positive definite matrices P_1, \dots, P_N , N matrices $F_j, G_j (j = 1, \dots, N)$, matrices L and R of appropriate dimensions and a positive real α that is sufficiently large, we have:

$$\min_{P_i, F_j, G_j, L, R} \left[\sum_{i=1}^{i=N} \text{Tr}(QP_i) + R(\delta + \sigma) \right] \tag{17}$$

Subject to

$$\begin{pmatrix} b(P_j - P_k) - \alpha F_j - \alpha F_j^T + I & -\alpha G_j - F_j + P_i & L^T A_i^T + D^T B_{ui}^T + \alpha L^T + F_j \\ -\alpha G_j - F_j^T + P_i^T & -G_j - G_j^T & G_j \\ A_i L + B_{ui} D + \alpha L + F_j^T & G_j^T & -L - L^T \end{pmatrix} < 0 \tag{18}$$

$$\begin{pmatrix} \sigma I_{n \times n} & D^T \\ D & I_{m \times m} \end{pmatrix} > 0 \tag{19}$$

$$\begin{pmatrix} \delta I_{n \times n} & I_{n \times n} \\ I_{n \times n} & L \end{pmatrix} > 0$$

$$P_i > 0 \tag{20}$$

For $i, j, k = 1, \dots, N$

The control gain is then given by $K = DL^{-1}$.

Proof. Let us consider (18); replacing D by KL and D^T by $L^T K^T$ in (18), we get:

$$\begin{pmatrix} b(P_j - P_k) - \alpha F_j - \alpha F_j^T + I & -\alpha G_j - F_j + P_i & L^T A_i^T + L^T K^T B_{ui}^T + \alpha L^T + F_j \\ -\alpha G_j - F_j^T + P_i^T & -G_j - G_j^T & G_j \\ A_i L + B_{ui} KL + \alpha L + F_j^T & G_j^T & -L - L^T \end{pmatrix} < 0 \tag{21}$$

In (21), replacing $A_i + B_{ui}K$ by A_i and $A_i^T + K^T B_{ui}^T$ by A_i^T , we get:

$$\begin{pmatrix} b(P_j - P_k) - \alpha F_j - \alpha F_j^T + I & -\alpha G_j - F_j + P_i & L^T A_i^T + \alpha L^T + F_j \\ -\alpha G_j - F_j^T + P_i^T & -G_j - G_j^T & G_j \\ A_i L + \alpha L + F_j^T & G_j^T & -L - L^T \end{pmatrix} < 0 \tag{22}$$

Multiplying (22) by θ_i , σ_j and β_k and summing up, respectively, for $i = 1 \dots N$, $j = 1..M$ and $k = 1..K$, we obtain:

$$\begin{pmatrix} b(P(\sigma) - P(\beta)) - \alpha F(\sigma) - \alpha F^T(\sigma) + I & -\alpha G(\sigma) - F(\sigma) + P(\theta) & L^T A^T(\theta) + \alpha L^T + F(\sigma) \\ -\alpha G(\sigma) - F^T(\sigma) + P^T(\theta) & -G(\sigma) - G^T(\sigma) & G(\sigma) \\ A(\theta)L + \alpha L + F^T(\sigma) & G^T(\sigma) & -L - L^T \end{pmatrix} < 0 \tag{23}$$

Multiplying the LMI condition (23) by $\begin{pmatrix} I & 0 & \alpha I \\ 0 & I & 0 \\ 0 & 0 & I \end{pmatrix} < 0$ on the left and its transpose on the right, where α is a positive real number, we get:

$$\begin{pmatrix} \dot{P}(\theta) + \alpha A(\theta)L + \alpha L^T A^T(\theta) + I & -F(\sigma) + P(\theta) & L^T A^T(\theta) - \alpha L + F(\sigma) \\ -F^T(\sigma) + P^T(\theta) & -G(\sigma) - G^T(\sigma) & G(\sigma) \\ A(\theta)L - \alpha L^T + F^T(\sigma) & G^T(\sigma) & -L - L^T \end{pmatrix} < 0 \tag{24}$$

where $P(\theta)$ is a positive and symmetric matrix called the Lyapunov candidate matrix.

We suppose that $\alpha L^T = P(\theta) = F(\sigma)$ and $G(\sigma) = \frac{P(\theta)}{\alpha}$, then, we get:

$$\begin{pmatrix} \dot{P}(\theta) + A(\theta)P(\theta) + P(\theta)A^T(\theta) + I & 0 & \frac{P(\theta)A^T(\theta)}{\alpha} \\ 0 & -\frac{2P(\theta)}{\alpha} & \frac{P(\theta)}{\alpha} \\ \frac{A(\theta)P(\theta)}{\alpha} & \frac{P(\theta)}{\alpha} & -L - L^T \end{pmatrix} < 0 \tag{25}$$

Applying the Schur complement on LMI (25),

$$\dot{P}(\theta) + A(\theta)P(\theta) + P(\theta)A^T(\theta) + I < -\frac{2}{4\alpha - 1} A^T(\theta)P(\theta)A(\theta) \tag{26}$$

For values of α that are sufficiently large, we get

$$\dot{P}(\theta) + A(\theta)P(\theta) + P(\theta)A^T(\theta) + I < 0 \tag{27}$$

(27) can be written

$$\dot{P}(\theta) + A(\theta)P(\theta) + P(\theta)A^T(\theta) < -I \tag{28}$$

Thus, we get the Lyapunov condition written for the LPV systems

$$\dot{P}(\theta) + A(\theta)P(\theta) + P(\theta)A^T(\theta) < 0 \tag{29}$$

For the proof of (19), see [24].

The approach presented above is used for the case of a boost DC–DC converter modeled based on an LPV polytopic formulation.

4. Synthesis of Improved LQR Controllers for DC–DC Boost Converters

4.1. Modeling

In this section, two different uncertainty models are shown. The same uncertain parameter $\theta(t)$ is employed. The uncertain parameter belongs to (4) and is such that its derivative verifies (5) and (6).

$$\theta(t) = \left[D', \frac{1}{D'}, \frac{1}{R'}, \frac{1}{D'^2 R'} \right] \tag{30}$$

Any matrix in this set can be obtained by:

$$A(\theta(t)), B_u(\theta(t)) = \theta_1(A_1, B_{u1}) + \theta_2(A_2, B_{u2}) + \theta_3(A_3, B_{u3}) + \theta_4(A_4, B_{u4}) \tag{31}$$

and the derivative of $\theta(t)$ satisfies the bound imposed in Section 2.

The first model is a simplification of P_{2009} , and it was first introduced in [25]. This model, which will be noted as P_{2011} , is based on a polytopic covering of the space in $\theta(t)$. Since the variables in $\theta(t)$ are not fully independent, a polytopic covering with fewer vertices can be derived. The result is a polytope with eight vertices instead of the 16 vertices in P_{2009} . Figure 3 shows P_{2011} and Table 1 defines its vertices.

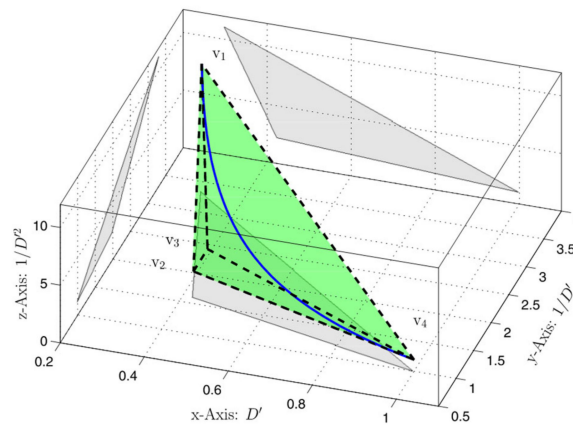


Figure 3. Plot of nonlinear uncertainty function ($f(D')$) (solid line) and reduced polytope P_{2011} (dashed line), as in [25]. The projections of the polytope are also shown in each respective plane.

Table 1. Vertices of the polytopic covering of P_{2011}

	D'	$\frac{1}{D}$	$\frac{1}{D^2 R}$	$\frac{1}{R}$
$\theta_1(t)$	0.3	1/0.3	1/0.9	1/10
$\theta_2(t)$	0.3	1/0.3	1/4.5	1/50
$\theta_3(t)$	0.425	1.6	2.25/10	1/10
$\theta_4(t)$	0.425	1.6	2.25/50	1/50
$\theta_5(t)$	0.425	2	2.25/10	1/10
$\theta_6(t)$	0.425	2	2.25/50	1/50
$\theta_7(t)$	1	1	1/10	1/10
$\theta_8(t)$	1	1	1/50	1/50

In order to test if the proposed synthesis approach can extend the region of stability of the system, we consider an extension of P_{2011} . This is a new model that considers an enlargement of the space in $\theta(t)$. Figure 4 shows the original P_{2011} polytope, and the novel enlarged one, noted as P_{2020} . The vertices of the model are shown in Table 2.

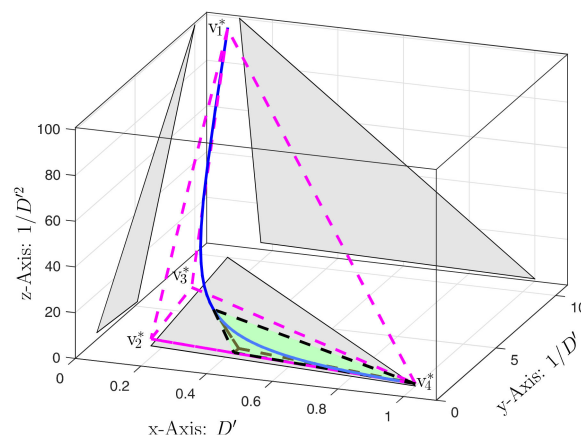


Figure 4. Plot of nonlinear uncertainty function ($f(D')$) (solid line) and proposed polytope P_{2020} for extended robustness (dashed pink line). The projections of the polytope are also shown in each respective plane. Note how P_{2020} compares with P_{2011} , which is shown here in black dashed lines and covers a much smaller parameter space.

Table 2. Vertices of the polytopic covering of P_{2020}

	D'	$\frac{1}{D'}$	$\frac{1}{D'^2 R}$	$\frac{1}{R}$
$\theta_1(t)$	0.1	1/0.1	1/0.1	1/10
$\theta_2(t)$	0.1	1/0.1	1/0.5	1/50
$\theta_3(t)$	0.165	1.8	3/10	1/10
$\theta_4(t)$	0.165	1.8	3/50	1/50
$\theta_5(t)$	0.165	5.2	1	1/10
$\theta_6(t)$	0.165	5.2	1/5	1/50
$\theta_7(t)$	1	1	1/10	1/10
$\theta_8(t)$	1	1	1/50	1/50

4.2. Synthesis Results

The same Q used in [7] is employed in the synthesis. The value of R was established using the proposed synthesis method with the old model P_{2009} . The objective was to obtain a controller that is equivalent to the one in [7], which is noted K_{eq} . That aim was achieved with $R = 1 \cdot 10^{-6}$.

4.2.1. Previous LQR Synthesis Method

Based on the LQR synthesis method given in [7], whose LMIs are shown in (6), three models have been tested: P_{2009} , P_{2011} and P_{2020} . The results are as follows:

- With P_{2009} : $K = \begin{bmatrix} -0.86 & -1.39 & 3159.54 \end{bmatrix}$.
- With P_{2011} : The set of LMIs is infeasible.
- With P_{2020} : The set of LMIs is infeasible.

4.2.2. Proposed LQR Synthesis Method

The synthesis with the novel conditions {17-18-19-20} results in the following controllers:

- With P_{2009} , $b = 1 \cdot 10^4$, $\alpha = 1 \cdot 10^5$, $R = 1 \cdot 10^{-6}$, the result is $K_{eq} = \begin{bmatrix} -0.55 & -0.89 & 1871.75 \end{bmatrix}$.

This controller achieves the same performance that can be obtained with controller K , but with a lower control effort (the gains in K_{eq} are smaller than those in K).

- With P_{2011} , $b = 1 \cdot 10^4$, $\alpha = 1 \cdot 10^5$, $R = 1 \cdot 10^{-6}$, the result is $K_{perf} = \begin{bmatrix} -0.46 & -1.49 & 4218 \end{bmatrix}$.
- With P_{2020} , $b = 1 \cdot 10^4$, $\alpha = 1 \cdot 10^5$, $R = 1 \cdot 10^{-5}$, the result is $K_{rob} = \begin{bmatrix} -0.01262 & 0.00095 & 9.607 \end{bmatrix}$.

5. Simulation Results

This section illustrates the properties of the different controllers K , K_{eq} , K_{perf} and K_{rob} . We have performed a set of PSIM [26] simulations of the switched DC–DC boost converter, according to Figure 1. The first set of simulations is useful to establish the performance of the controllers, by analyzing the response of the converter with respect to changes in the output current. The second set aims to establish the robustness of the different controllers when there is a change in the operating point, by modifying the supply voltage.

First, the waveforms of the simulations with changes in the load are grouped in Figure 5. The top waveforms in each subfigure correspond to the output voltage $v_0(t)$, whereas the bottom waveform represents the output current $i_{load}(t)$. In all simulations, the converter load is initially the nominal value $R = 25\Omega$. At time $t = 1$ ms, the load changes to $R = 10\Omega$, which is the maximum load allowed by design in all polytopes. The load returns to $R = 25\Omega$ at $t = 6$ ms.

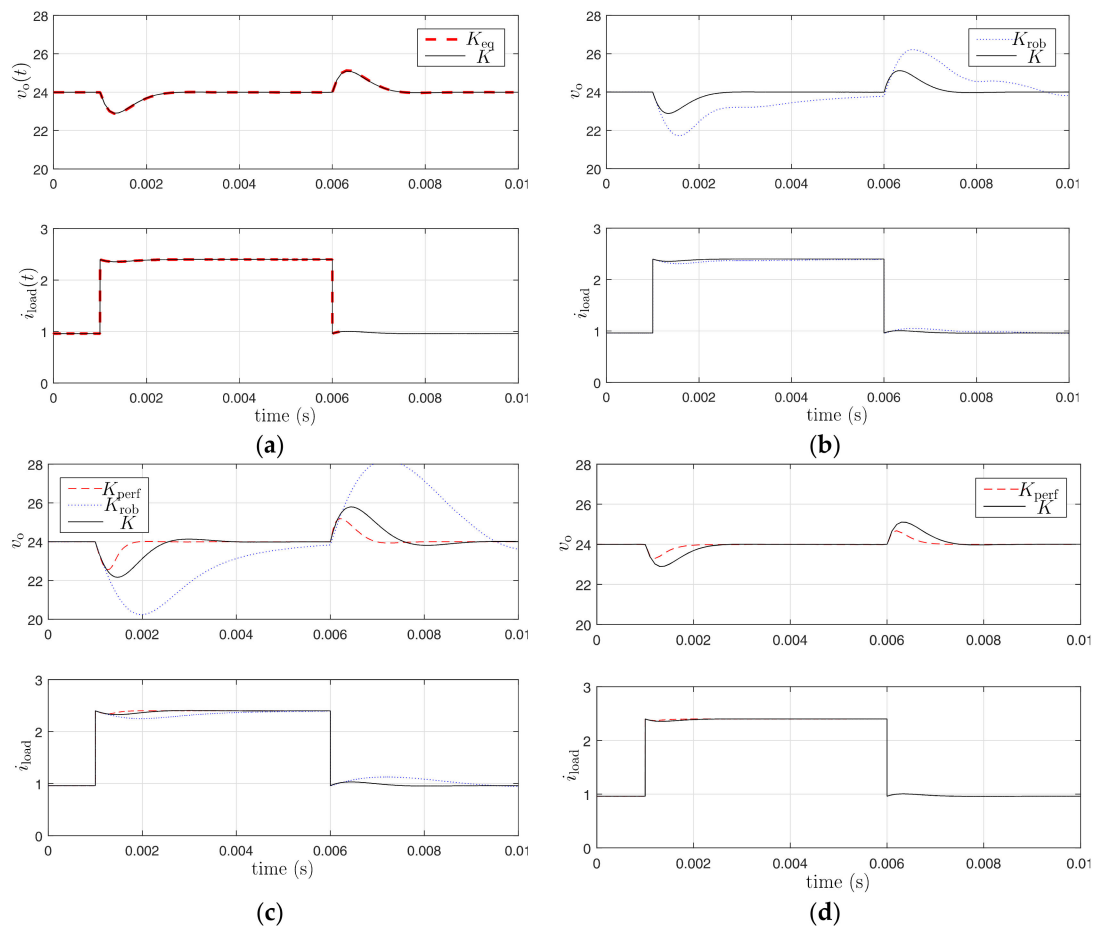


Figure 5. Simulated transient of the boost converter under a load step transient with the robust LQR controllers K (solid line), K_{eq} (thick dashed line), K_{perf} (dashed line) and K_{rob} (dotted line); (a–c) show the transient when $V_g = 12\text{ V}$ and the operating point duty cycle is $D' = 0.5$; (d) shows the transient when $V_g = 7.2\text{ V}$ and the operating point duty cycle is $D' = 0.3$.

As a baseline for the comparison, Figure 5a shows the performance of controller K , as in [7], and the performance of controller K_{eq} obtained with the proposed method and the same polytope used in [7], P_{2009} . It can be seen that the disturbance rejection properties and the settling time are nearly identical. In contrast, Figure 5b shows a comparison with controller K_{perf} , which exhibits a tight regulation of the output voltage, such that the maximum error of $v_o(t)$ and its settling time are reduced to approximately one half of what is achieved with K . As expected, the robust controller K_{rob} presents loose regulation and a slower response, as shown in Figure 5c, when compared to K .

Note that Figure 5a–c shows the response at the nominal operating point, when $v_g(t) = 12\text{ V}$ and $D' = 0.5$. In order to evaluate the performance at a different operating point, Figure 5d shows the response of K , K_{perf} and K_{rob} under an input voltage variation of -40% , such that the operating point is now $D' = 0.3$. Again, K_{perf} is the controller that achieves excellent regulation properties, maintaining its robustness in the expected region of operation.

If K_{perf} is the controller that demonstrates that the proposed method can be used to improved regulation while maintaining the same robustness properties, K_{rob} is the controller that demonstrates that the method can also be employed to enlarge the stability region. Figure 6 shows the waveforms of the simulations in which the input voltage is stepped, such that the operating point of the converter is modified in time. Figure 6a shows a voltage step of -40% , which corresponds to a step in the duty cycle from $D' = 0.5$ to $D' = 0.3$ ($D = 0.7$). Since all polytopes considered such a region, the three controllers maintain the stability, with K_{perf} exhibiting the best regulation performance. Figure 6b shows a similar

step in the input voltage, but now the input voltage decreases down to $v_g(t) = 2.4V$, such that the operating point duty cycle moves from $D' = 0.3$ to $D' = 0.1$. The method proposed in [7] did not allow us to consider such a large range of operating point uncertainty, whereas the proposed method resulted in controller K_{rob} . As can be seen in the figure, K_{rob} is the only controller that successfully maintains stability under those conditions, exhibiting excellent stability properties.

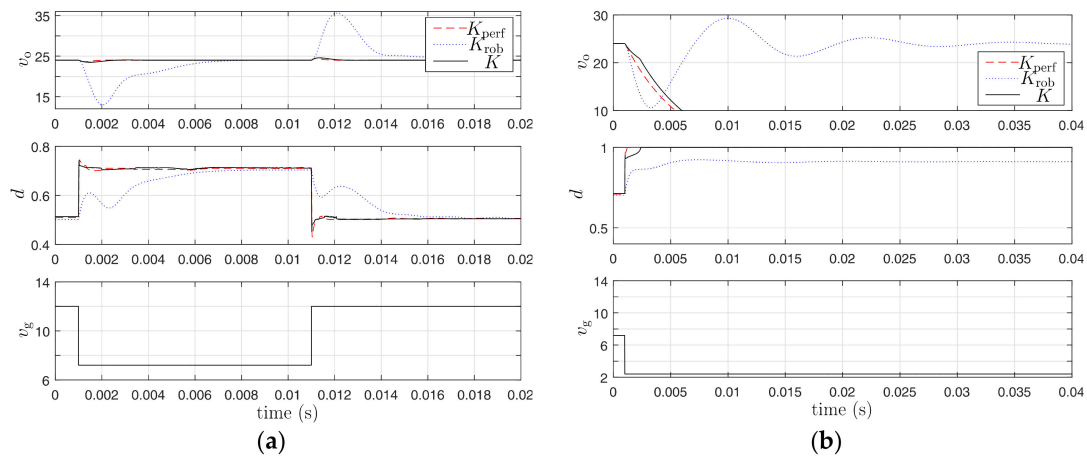


Figure 6. Simulated transient of the boost converter, in the presence of an input voltage disturbance, with the robust LQR controllers K (solid line), K_{perf} (dashed line) and K_{rob} (dotted line). (a) The input voltage steps down to 7.2 V, which corresponds to $D = 0.7$. All controllers consider such a change of operating point and maintain the stability. (b) The input voltage steps down to 2.4 V, which corresponds to $D = 0.9$. Only controller K_{rob} maintains the stability of the regulation.

It is worth noting that the transient shown in Figure 6b shows the saturation of the duty cycle at 100% with the unstable controllers. Although the modeling of that nonlinearity is out of the scope of this paper, this aspect has been treated in the specific context of switched-mode power converters in [27].

Finally, Figure 7 depicts the waveforms of the converter startup, with the three controllers K , K_{perf} and K_{rob} . The input voltage is $V_g = 12$ V and the voltage reference ramps up from 12 V to 24 V at $t = 0$, with a rate of change of 2400 V/s. It can be observed that the three controllers operate inside the expected range of operation and stabilize the converter.

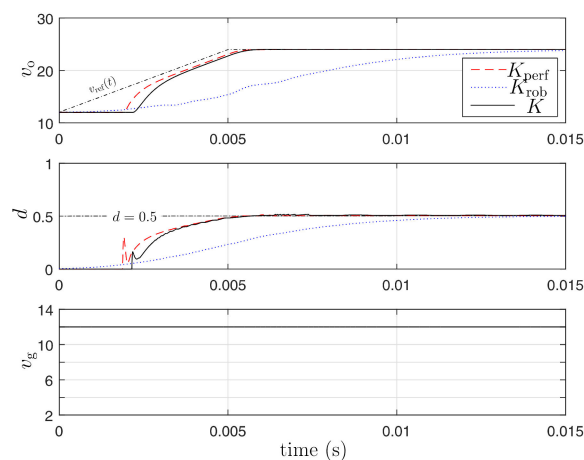


Figure 7. Simulated transient of the boost converter during startup with $V_g = 12$ V, for the three controllers K (solid line), K_{perf} (dashed line) and K_{rob} (dotted line). Top waveforms: output voltage. Middle waveforms: duty cycle. Bottom waveform: input voltage.

6. Conclusions

The numerical synthesis of robust LQR controllers for PWM DC–DC converters by means of LMIs has suffered from the conservativeness of the methods based on quadratic stability, since a single Lyapunov function is employed for the entire uncertainty region and because the uncertain parameters are assumed to change arbitrarily fast. This paper proposes a new method to synthesize robust LQR controllers. The method employs parameter-dependent Lyapunov functions and allows us to consider the rate of change of the uncertain parameters.

The method has been employed to synthesize LQR controllers for a PWM DC–DC boost converter. With that aim, the paper has reviewed two uncertainty models of the boost converter that were proposed in the past. In addition, it has introduced an enlarged version of one of them, with the objective to obtain stability for a very large region of uncertain parameters. While the conventional synthesis methods fail to obtain feasible solutions with these uncertainty models, the proposed method has been demonstrated to be useful in achieving better regulation performance or improved robustness.

Author Contributions: N.A. and C.O. conceptualized the research; N.A. and C.O. conceived the methodology and the formal analysis; C.O. completed the investigation and carried out validation tasks; N.A. and C.O. wrote the original draft, reviewed and edited the final paper. All authors have read and agreed to the published version of the manuscript.

Funding: The research leading to these results has received funding from the Spanish Ministry of Economy and Competitiveness under grant DPI2017-84572-C2-1-R, and also from the Research Unit of System Analysis and Control, National School Engineering of Tunis, Tunisian Ministry of Scientific Research and Higher Education.

Conflicts of Interest: The authors declare no conflict of interest.

References

1. Middlebrook, R.D.; Čuk, S. A general unified approach to modelling switching-converter power stages. *Int. J. Electron.* **1977**, *42*, 521–550. [[CrossRef](#)]
2. Erickson, R.W.; Maksimović, D. *Fundamentals of Power Electronics*; Springer: Cham, Switzerland, 2001.
3. Deisch, C. Simple switching control method changes power converter into a current source. *IEEE Power Electron. Spec. Conf.* **1978**, 300–306. [[CrossRef](#)]
4. Capel, A.; Ferrante, G.; O’Sullivan, D.; Weinberg, A. Application of the injected current model for the dynamic analysis of switching regulators with the new concept of LC3 modulator. *IEEE Power Electron. Spec. Conf.* **1978**, 135–147. [[CrossRef](#)]
5. Montagner, V.; Peres, P. Robust pole location for a DC-DC converter through parameter dependent Control In Proceedings of the 2003 International Symposium on Circuits and Systems, ISCAS 2003. Bangkok, Thailand, 25–28 May 2003; Volume 3, pp. 351–354.
6. Olalla, C.; Leyva, R.; el Aroudi, A.; Garcés, P.; Queinnec, I. LMI robust control design for boost PWM converters. *IET Power Electron.* **2010**, *3*, 75. [[CrossRef](#)]
7. Olalla, C.; Leyva, R.; el Aroudi, A.; Queinnec, I. Robust LQR Control for PWM Converters: An LMI Approach. *IEEE Trans. Ind. Electron.* **2009**, *56*, 2548–2558. [[CrossRef](#)]
8. Gabe, I.J.; Montagner, V.F.; Pinheiro, H. Design and Implementation of a Robust Current Controller for VSI Connected to the Grid Through an LCL Filter. *IEEE Trans. Power Electron.* **2009**, *24*, 1444–1452. [[CrossRef](#)]
9. Olalla, C.; Queinnec, I.; Leyva, R.; el Aroudi, A. Optimal State-Feedback Control of Bilinear DC–DC Converters With Guaranteed Regions of Stability. *IEEE Trans. Ind. Electron.* **2011**, *59*, 3868–3880. [[CrossRef](#)]
10. Maccari, L.A.; Massing, J.R.; Schuch, L.; Rech, C.; Pinheiro, H.; Oliveira, R.C.L.F.; Montagner, V.F. LMI-Based Control for Grid-Connected Converters With LCL Filters Under Uncertain Parameters. *IEEE Trans. Power Electron.* **2013**, *29*, 3776–3785. [[CrossRef](#)]
11. Albea-Sanchez, C.; Garcia, G. Robust hybrid control law for a boost inverter. *Control Eng. Pr.* **2020**, *101*, 104492. [[CrossRef](#)]
12. Sferlazza, A.; Albea-Sanchez, C.; Garcia, G. A hybrid control strategy for quadratic boost converters with inductor currents estimation. *Control Eng. Pr.* **2020**, *103*, 104602. [[CrossRef](#)]
13. Olalla, C.; Leyva, R.; Queinnec, I.; Maksimovic, D. Robust Gain-Scheduled Control of Switched-Mode DC–DC Converters. *IEEE Trans. Power Electron.* **2012**, *27*, 3006–3019. [[CrossRef](#)]

14. Aouani, N.; Salhi, S.; Ksouri, M.; Garcia, G. H₂ analysis for LPV systems by parameter-dependent Lyapunov functions. *IMA J. Math. Control Inf.* **2011**, *29*, 63–78. [[CrossRef](#)]
15. Aouani, N.; Salhi, S.; Garcia, G.; Ksouri, M. New robust stability and stabilizability conditions for linear parameter time varying polytopic systems. In Proceedings of the 2009 3rd International Conference on Signals, Circuits and Systems (SCS), Medenine, Tunisia, 6–8 November 2009; pp. 1–6.
16. Xie, W. H₂ gain scheduled state feedback for LPV system with new LMI formulation. *IEEE Proc. Control Theory Appl.* **2005**, *152*, 693–697. [[CrossRef](#)]
17. Cao, Y.-Y.; Lin, Z. A Descriptor System Approach to Robust Stability Analysis and Controller Synthesis. *IEEE Trans. Autom. Control* **2004**, *49*, 2081–2084. [[CrossRef](#)]
18. Wu, F.; Grigoriadis, K.M. LPV Systems with parameter-varying time delays: Analysis and Control. *Automatica* **2001**, *37*, 221–229. [[CrossRef](#)]
19. Wu, F.; Packard, A. LQG control design for LPV systems. In Proceedings of the 1995 American Control Conference—ACC'95, Seattle, WA, USA, 21–23 June 1995.
20. Rödönyi, G.; Bokor, J. LQG control of LPV systems with parameter-dependent Lyapunov function. In Proceedings of the 10th Mediterranean Conference, on Control and Automation—MED2002, Lisbon, Portugal, 9–12 July 2002.
21. Osório, C.; Koch, G.; Oliveira, R.C.; Montagner, V.F. A practical design procedure for robust H₂ controllers applied to grid-connected inverters. *Control Eng. Pr.* **2019**, *92*. [[CrossRef](#)]
22. Liu, Z.; Theilliol, F.; Gu, D.; He, Y.; Yang, L.; Han, J. State Feedback Controller Design for Affine Parameter-Dependent LPV systems. *IFAC PapersOnLine* **2017**, *50*, 9760–9765. [[CrossRef](#)]
23. Ilka, A.; Vesely, V. Robust LPV-based infinite horizon LQR design. In Proceedings of the 2017 21st International Conference on Process Control (PC), Štrbské Pleso, Slovakia, 6–9 June 2017; pp. 86–91.
24. Tarbouriech, S.; Souères, P.; Gao, B. A multicriteria image-based controller based on a mixed polytopic and norm-bounded representation of uncertainties. In Proceedings of the 44th IEEE Conference on Decision and Control, Seville, Spain, 12–15 December 2005; pp. 5385–5390.
25. Olalla, C.; Queinnec, I.; Leyva, R.; el Aroudi, A. Robust optimal control of bilinear DC–DC converters. *Control Eng. Pr.* **2011**, *19*, 688–699. [[CrossRef](#)]
26. PSIM User Manual, Powersim Inc. 2003. Available online: <https://powersimtech.com/drive/uploads/2019/04/PSIM-user-manual.pdf> (accessed on 30 August 2020).
27. Olalla, C.; Leyva, R.; el Aroudi, A.; Queinnec, I.; Tarbouriech, S. Hinf Control of DC-DC Converters with Saturated Inputs. In Proceedings of the IEEE Annual Conference on Industrial Electronics IECON, Porto, Portugal, 3–5 November 2009.

Publisher's Note: MDPI stays neutral with regard to jurisdictional claims in published maps and institutional affiliations.



© 2020 by the authors. Licensee MDPI, Basel, Switzerland. This article is an open access article distributed under the terms and conditions of the Creative Commons Attribution (CC BY) license (<http://creativecommons.org/licenses/by/4.0/>).